Journal of Magnetism and Magnetic Materials 615 (2025) 172792

Contents lists available at ScienceDirect

Journal of Magnetism and Magnetic Materials

journal homepage: www.elsevier.com/locate/jmmm

Research article

Spin gapped metals: A novel class of materials for multifunctional spintronic devices

E. Şaşıoğlu [a], M. Tas [b], S. Ghosh [c,d], W. Beida [e,f], B. Sanyal [d], S. Blügel [f], I. Mertig [a], I. Galanakis [g,*]

[a] Institute of Physics, Martin Luther University Halle-Wittenberg, 06120, Halle (Saale), Germany
[b] Department of Physics, Gebze Technical University, 41400 Kocaeli, Turkey
[c] Department of Physics, Central University of Kashmir,Tulmulla, Ganderbal, Jammu and Kashmir, 191131, India
[d] Department of Physics and Astronomy, Uppsala University, 75120, Uppsala, Sweden
[e] Physics Department, RWTH Aachen University, 52062, Aachen, Germany
[f] Peter Grünberg Institut, Forschungszentrum Jülich and JARA, 52425 Jülich, Germany
[g] Department of Materials Science, School of Natural Sciences, University of Patras, 26504, Patras, Greece

ARTICLE INFO

Keywords:
Heusler compounds
Ab-initio calculations
Density functional theory calculations
Gapped metals
Magnetic materials

ABSTRACT

Gapped metals, a recently proposed class of materials, possess a band gap slightly above or below the Fermi level, behaving as intrinsic p- or n-type semiconductors without requiring external doping. Inspired by this concept, we propose a novel material class: "spin gapped metals". These materials exhibit intrinsic p- or n-type character independently for each spin channel, similar to dilute magnetic semiconductors but without the need for transition metal doping. A key advantage of spin gapped metals lies in the absence of band tails that exist within the band gap of conventional p- and n-type semiconductors. Band tails degrade the performance of devices like tunnel field-effect transistors (causing high subthreshold slopes) and negative differential resistance tunnel diodes (resulting in low peak-to-valley current ratios). Here, we demonstrate the viability of spin gapped metals using first-principles electronic band structure calculations on half-Heusler compounds. Our analysis reveals compounds displaying both gapped metal and spin gapped metal behavior, paving the way for next-generation multifunctional devices in spintronics and nanoelectronics.

1. Introduction

An essential challenge in materials science involves uncovering materials possessing unique characteristics that can bolster device performance. Thermoelectricity, which involves converting heat into electricity via the Seebeck effect, stands as a pivotal phenomenon in contemporary technology, enabling the harnessing of waste heat from both industrial and household processes [1,2]. While doped semiconductors are traditionally favored for thermoelectric applications, recent suggestions propose a new category of metals termed "gapped metals" as potential substitutes for doped semiconductors [3–5]. As illustrated in Fig. 1(a–c), the density of states (DOS) for these gapped metals reveal a semiconductor-like gap, which distinguishes them from conventional metals. Specifically, the Fermi level intersects either the valence band, resulting in an excess of holes (p-type gapped metals), or the conduction band, leading to an excess of electrons (n-type gapped metals). A key advantage of gapped metals lies in the absence of band tails, which originates from the strong doping and doping fluctuations in conventional p-/n-type semiconductors and they have been studied in detail by many authors using different approaches [6–12]. Band tails degrade the performance of devices like tunnel field-effect transistors (FETs) with increased subthreshold slope (SS) and negative differential resistance (NDR) tunnel diodes with lowered peak-to-valley current ratio.

Gapped metals, a subclass of "cold metals", share many similar characteristics [13]. Cold metals have garnered significant interest for their potential in next-generation electronics, particularly devices like NDR tunnel diodes [14] and steep-slope FETs. When used as source and drain electrodes in FETs, gapped metals, similar to cold metals, can filter the transmission of high-energy electrons in the subthreshold region, leading to sub-60 mV/dec SS values and reduced leakage current in the off-state [15–19]. Furthermore, gapped metals, like cold metals, can be employed in metal–semiconductor Schottky barrier diodes instead of the normal metals to surpass the thermionic emission limit, typically characterized by an ideality factor (η) of 1 at room temperature.

* Corresponding author.
E-mail addresses: ersoy.sasioglu@physik.uni-halle.de (E. Şaşıoğlu), galanakis@upatras.gr (I. Galanakis).

https://doi.org/10.1016/j.jmmm.2025.172792
Received 5 December 2024; Received in revised form 8 January 2025; Accepted 10 January 2025
Available online 16 January 2025
0304-8853/© 2025 The Authors. Published by Elsevier B.V. This is an open access article under the CC BY license (http://creativecommons.org/licenses/by/4.0/).

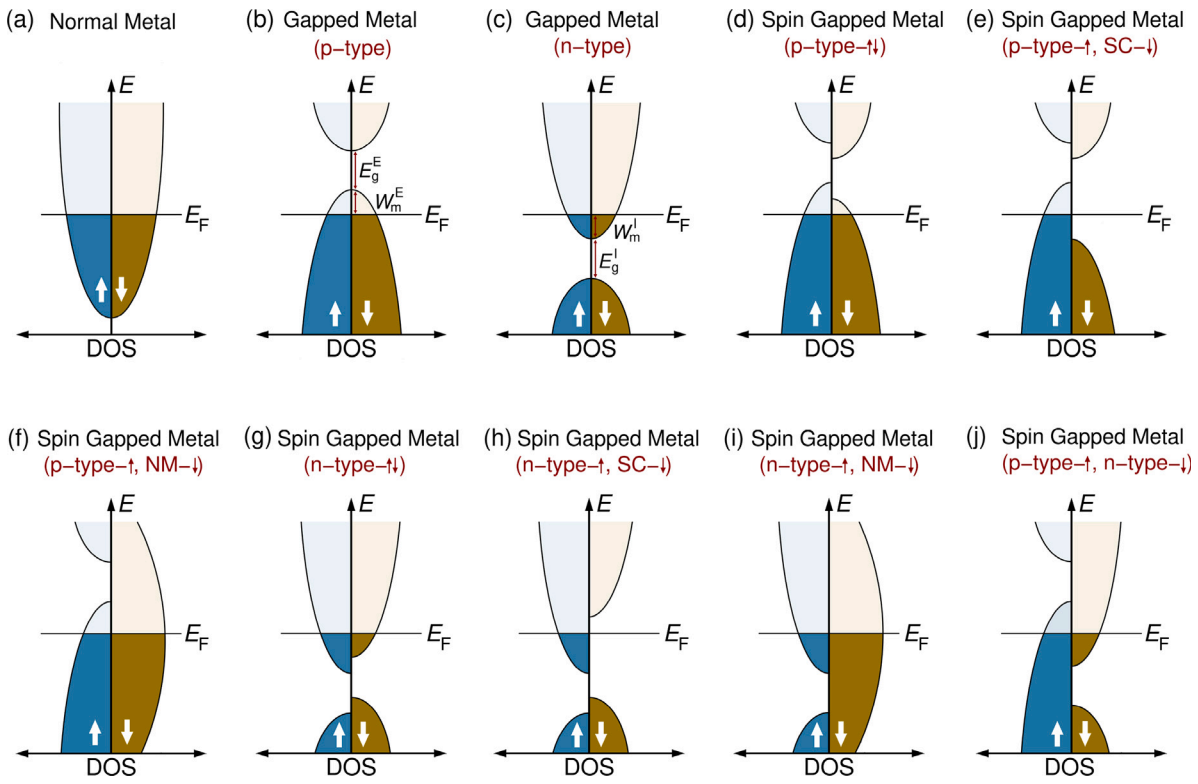


Fig. 1. Schematic representation of the density of states (DOS) of a normal metal (a), gapped metals (b–c), and spin gapped metals (d–j). The arrows represent the two possible spin directions. The horizontal line depicts the Fermi level E_F. NM stands for normal-metal and SC for semiconductor.

These advancements pave the way for the development of low-power nanoelectronic circuits [20].

In this Article, we introduce the term 'spin gapped metals', extending the concept of gapped metals to encompass magnetic materials. This terminology encapsulates the distinct spin-dependent electronic band structures of these materials. Such an extension would result in a diverse range of behaviors stemming from the distinct characteristics of each metal. Seven distinct scenarios are presented in Fig. 1(d–j) to illustrate this concept. By combining n- or p-type gapped metallic behavior for the spin-up electronic band structure with various behaviors such as normal metallic, typical semiconducting, or n(p)-type gapped metallic behavior in the spin-down electronic band structure, a broader range of implications for device applications could be achieved. Analogous to how gapped metals are seen as counterparts to doped semiconductors, one might view spin gapped metals as counterparts to diluted magnetic semiconductors [21–24], such as Mn-doped GaAs, without requiring the incorporation of magnetic atoms through doping.

2. Results and discussion

Gapped metals and spin gapped metals can be qualitatively described by four key electronic structure parameters as shown on the schematic density of states in Fig. 1. These parameters include the internal band gap (E_g^I), the external band gap (E_g^E) and internal (external) metallic bandwidth W_m^I (W_m^E). W_m^E represents the energy difference between the Fermi level and the valence band maximum for p-type gapped and spin gapped metals, while W_m^I represents the energy difference between the conduction band minimum and the Fermi level for n-type materials. The importance of W_m^E is evident in FETs when gapped metals are used as source electrodes, as demonstrated in reference [16] for p-type $NbTe_2$-based transistors. A smaller W_m^E value translates to a lower SS for the transistor, leading to reduced energy consumption. FETs designed with both source and drain electrodes composed of p-type gapped metals (or cold metals) are predicted to exhibit not only transistor functionality but also the gate-voltage tunable NDR effect [25]. The spin degree of freedom in spin gapped metals opens exciting possibilities for the development of multifunctional devices, which we will comment on later in this paper.

The recently proposed concept of "gapped metals" [4], although new, has already been observed in many materials reported earlier [26–29]. This newfound understanding has ignited renewed interest in identifying materials that exemplify this promising class [3,5]. Similarly, materials exhibiting spin gapped metal-like behavior might exist in previously published works, but have not been categorized as such due to the lack of a suitable framework. In this work, we address this gap by extending the concept of gapped metals to magnetic materials, introducing the term "spin gapped metals". This framework allows for the classification of new materials based on their spin-dependent electronic structures. Motivated by our recent discovery of spin-polarized two-dimensional electron/hole gas at the interfaces of semiconducting 18-valence electron half-Heusler compounds (also known as semi-Heusler compounds), which displayed spin gapped metal-like interface states [30], we aim to explore 17-valence electron and 19-valence electron half-Heusler compounds as potential candidates for exhibiting spin gapped metal behavior. The so-called 18-valence electrons half-Heusler compounds, such as CoTiSb, FeVSb, or NiTiSn, are renowned semiconductors exhibiting remarkably high-temperature thermoelectric properties [30–38]. Seeking spin gapped metals within the half-Heusler compounds, deviating from the 18-valence electrons semiconducting Heusler compounds seems a logical step.

The choice to search for spin gapped metals among the Heusler compounds is natural since the latter constitute a vast family of intermetallic compounds, currently comprising over 2000 members [42–44]. Within this family, numerous novel behaviors have been both experimentally and computationally identified, rendering them appealing for a wide array of device applications. These behaviors include half-metallicity [45], spin gapless semiconducting behavior [38,46,47], spin-filtering [48], and more. Their adaptability regarding element substitution drives ongoing research in this field, and extended databases

Table 1
Lattice constants a_0, valence electron number Z_T, sublattice and total magnetic moments, spin polarization at the Fermi level (SP, see text for definition), spin gap type per spin direction, the distance of the Fermi level from the edge of the band which it crosses $W_m^{LE(\uparrow/\downarrow)}$ (see text for more details), energy gap per spin direction $E_g^{LE(\uparrow/\downarrow)}$, formation energy ($E_{form}$), and convex hull distance energy (ΔE_{con}) for the compounds under study. The a_0, E_{form} and ΔE_{con} values are taken from the Open Quantum Materials Database [39–41].

Compound XYZ	a_0 (Å)	Z_T	m_X (μ_B)	m_Y (μ_B)	m_{total} (μ_B)	SP (%)	Spin gap type	$W_m^{LE(\uparrow/\downarrow)}$ (eV)	$E_g^{LE(\uparrow/\downarrow)}$ (eV)	E_{form} (eV/at.)	E_{con} (eV/at.)
Spin gapped metals											
FeTiSb	5.94	17	−1.45	0.53	−0.95	68	p-type-↑/p-type-↓	0.58/0.12	0.47/0.76	−0.39	0.04
FeZrSb	6.15	17	−1.34	0.34	−1.00	100	p-type-↑/SC-↓	0.64	0.90/	−0.45	0.03
FeHfSb	6.11	17	−1.26	0.27	−1.00	100	p-type-↑/SC-↓	0.60	1.28/	−0.39	0.00
FeVSn	5.87	17	−1.85	1.03	−0.88	36	NM-↑/p-type-↓	0.15	0.59	0.06	0.18
FeNbSn	6.00	17	−1.38	0.40	−1.00	100	p-type-↑/SC-↓	0.70	0.16	−0.10	0.06
FeTaSn	5.99	17	−1.29	0.32	−1.00	100	p-type-↑/SC-↓	0.70	0.56/	−0.06	0.09
CoTiSn	5.93	17	−0.42	−0.45	−0.94	74	p-type-↑/p-type-↓	0.37/0.06	0.94/0.84	−0.38	0.07
CoZrSn	6.15	17	−0.67	−0.18	−0.95	81	p-type-↑/p-type-↓	0.41/0.09	0.97/0.74	−0.46	0.05
CoHfSn	6.11	17	−0.55	−0.15	−0.79	66	p-type-↑/p-type-↓	0.38/0.24	1.02/0.71	−0.43	0.04
RhTiSn	6.17	17	−0.07	−0.73	−0.87	70	p-type-↑/p-type-↓	0.56/0.09	0.63/0.65	−0.60	0.06
IrTiSn	6.20	17	−0.08	−0.61	−0.76	33	p-type-↑/p-type-↓	0.45/0.13	0.71/0.67	−0.61	0.02
NiZrIn	6.22	17	−0.11	−0.31	−0.55	53	p-type-↑/p-type-↓	0.49/0.34	0.30/0.30	−0.31	0.12
PtTiIn	6.24	17	−0.04	−0.84	−1.00	100	p-type-↑/SC-↓	0.45/	0.78/	−0.56	0.10
CoVSb	5.81	19	−0.33	1.41	1.00	100	n-type-↑/SC-↓	0.79/	0.35/	−0.19	0.07
RhVSb	6.07	19	−0.21	1.33	1.00	100	n-type-↑/SC-↓	0.87/	0.25/	−0.31	0.10
PdTiSb	6.24	19	−0.04	0.98	0.89	87	n-type-↑/n-type-↓	0.59/0.19	0.49/0.41	−0.51	0.09
PtTiSb	6.26	19	−0.05	1.05	0.99	93	n-type-↑/n-type-↓	0.53/0.02	0.74/0.78	−0.65	0.11
NiVSn	5.87	19	−0.03	1.15	1.00	100	n-type-↑/SC-↓	0.41/	0.67/	−0.08	0.15
NiVSb	5.88	20	0.03	2.12	2.00	100	n-type-↑/SC-↓	0.68/	0.80/	−0.12	0.13
CuVSb	6.06	21	0.04	3.04	2.95	40	n-type-↑/NM-↓	1.44/	0.15/	0.21	0.24
Gapped metals											
NiHfIn	6.16	17	0.00	0.00	0.00	0	p-type-↑/p-type-↓	0.45/0.45	0.32/0.32	−0.26	0.17
NiTiSb	5.93	19	0.00	0.00	0.00	0	n-type-↑/n-type-↓	0.69/0.69	0.61/0.61	−0.52	0.05
NiZrSb	6.15	19	0.00	0.00	0.00	0	n-type-↑/n-type-↓	0.88/0.88	0.75/0.75	−0.62	0.03
NiHfSb	6.10	19	0.00	0.00	0.00	0	n-type-↑/n-type-↓	0.96/0.96	0.67/0.67	−0.53	0.06
NiNbSn	6.00	19	0.00	0.00	0.00	0	n-type-↑/n-type-↓	0.73/0.73	0.88/0.88	−0.19	0.09

were built using the first-principles calculations resulting in the prediction of hundreds of new Heusler compounds which were later grown experimentally [31,45,47,49–55].

To pursue the objective of identifying spin gapped metals, we conducted a search in the Open Quantum Materials Database (OQMD) [39] and identified 25 half-Heusler compounds, as outlined in Table 1. These compounds typically possess 17 or 19 valence electrons per unit cell, though some exceptions with 20 or 21 valence electrons exist. Our initial criterion for selecting compounds for the study was their formation energy, E_{form}, which we aimed to be negative, with a few exceptions like FeVSn and CuVSb included for completeness, as their values are close to zero despite being positive. However, negative E_{form} alone does not guarantee stability. The convex hull distance ΔE_{con}, which represents the energy difference between the studied structure and the most stable phase or a mixture of phases, is also crucial. Typically, a value less than 0.2 eV/atom is desired to facilitate the growth of a material in a metastable form, such as a thin film or a nanostructure. All materials selected from the OQMD for our study exhibit ΔE_{con} values less than the cutoff of 0.2 eV/atom, except for CuVSb, which has a value of 0.24 eV/atom. The formation and convex hull distance energies from the OQMD are detailed in Table 1.

The bulk half-Heusler compounds XYZ that we consider in this work crystallize in the cubic $C1_b$ lattice structure (see figure 2 in reference [45]). The space group is the $F\bar{4}3m$ and actually consists of four interpenetrating f.c.c. sublattices; one is empty and the other three are occupied by the X, Y, and Z atoms. The unit cell is an f.c.c. one with three atoms as a basis along the long diagonal of the cube: X at (0 0 0), Y at $(\frac{1}{4}\ \frac{1}{4}\ \frac{1}{4})$ and Z at $(\frac{3}{4}\ \frac{3}{4}\ \frac{3}{4})$ in Wyckoff coordinates. We adopted the lattice constants calculated in the OQMD for all twenty-five materials [39–41], and we present them in the second column in Table 1. Our tests show that the lattice constants presented in OQMD, where the Perdew–Burke–Ernzerhof (PBE) functional has been used for the exchange–correlation potential [56], differ less than 1% from the PBE equilibrium ones calculated with the electronic band structure method employed in the current study.

The ground-state first-principles electronic band-structure calculations for all studied compounds were carried out using the QuantumATK software package [57,58]. We use linear combinations of atomic orbitals (LCAO) as a basis set together with norm-conserving PseudoDojo pseudopotentials [59]. The PBE parameterization to the generalized-gradient-approximation of the exchange–correlation potential is employed [56]. Note that due to the metallic character of the compounds under study, the GGA provides a more accurate description of the ground state properties concerning more complex hybrid functionals [37,60]. For determination of the ground-state properties of the bulk compounds, we use a 16 × 16 × 16 Monkhorst–Pack **k**-point grid [61].

Our calculations do not account for the spin–orbit coupling. This interaction is anticipated to introduce states within the energy gap, particularly in materials exhibiting half-metallic ferromagnetism. These materials are characterized by a minority-spin band gap encompassing the Fermi level, while the majority-spin band displays metallic behavior. However, studies by Mavropoulos et al. [62] utilizing relativistic first-principles calculations have demonstrated that the influence of spin–orbit coupling is negligible in NiMnSb half-metallic Heusler compound. This finding was further generalized by Mavropoulos et al. [63] to encompass not only half-metals but also near-half-metallic materials such as PdMnSb and PtMnSb. These materials maintain nearly 100% spin polarization at the center of the energy gap. The authors in Ref. [63] explained this behavior using perturbation theory. They showed that DOS exhibits a quadratic dependence on the strength of spin–orbit coupling. Furthermore, the spin-down DOS weakly mirrors the spin-up DOS, resulting in a minimal impact of spin–orbit coupling.

Our search resulted in twenty-five half-Heusler compounds which fullfil the criteria discussed above and our calculations indicate that are either gapped or spin gapped metals. In Table 1 we have compiled our results. We have five compounds that are non-magnetic and belong to the gapped metals. Among them, only NiHfIn has 17 valence electrons per unit cell while the other four have 19 valence electrons. Since the 18 valence-electrons compounds are semiconductors, one would expect NiHfIn to be a p-type gapped metal with the Fermi level crossing the valence band, and the rest n-type gapped metals with the Fermi level crossing the conduction band. Our calculated band structures confirm these predictions as shown in Table 1. In Table 1 we also include the distance of the Fermi level from the edge of the band which it crosses,

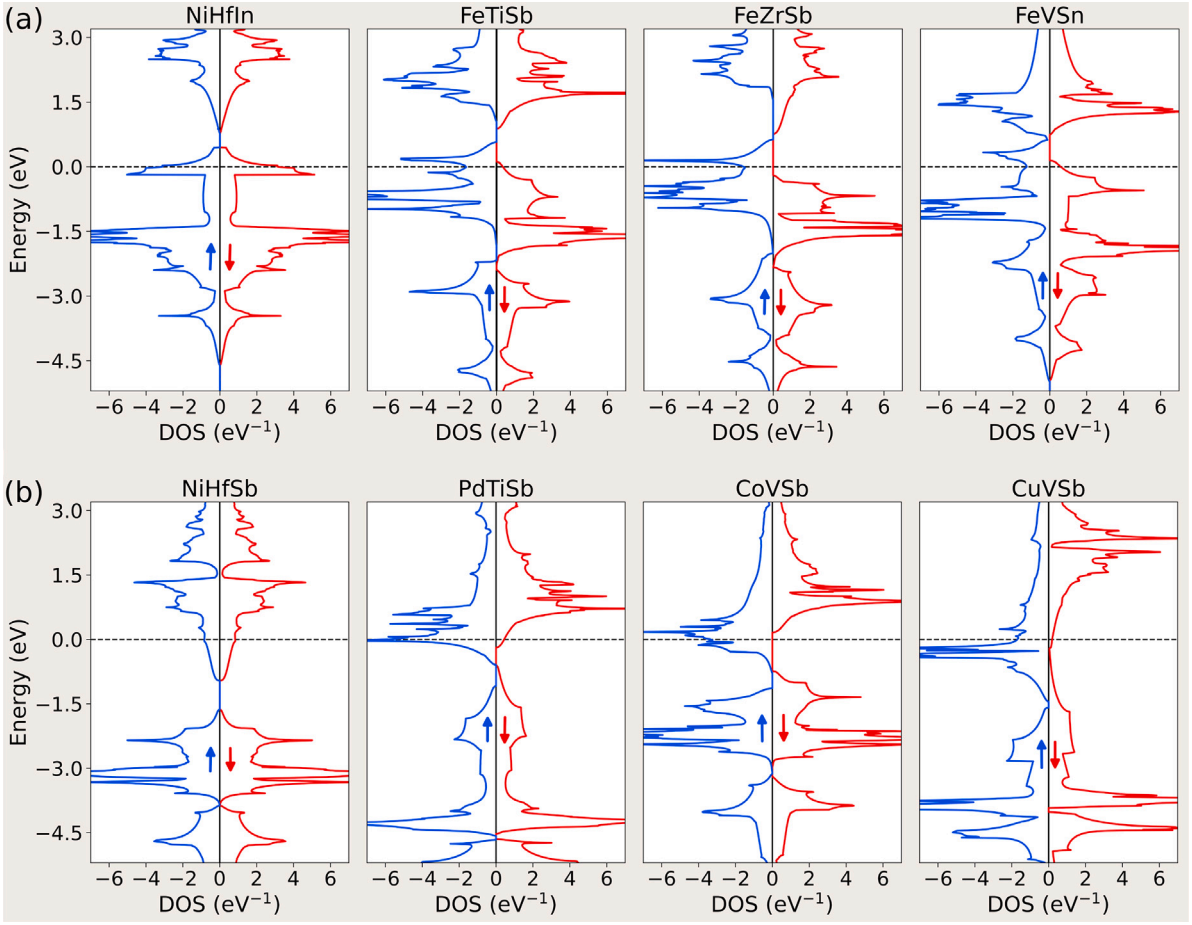


Fig. 2. Spin-resolved total density of states for selected gapped and spin gapped half-Heusler compounds. The zero energy corresponds to the Fermi level. Arrows depict the spin direction.

$W_m^{I,E(\uparrow/\downarrow)}$, The $W_m^{I,E(\uparrow/\downarrow)}$ value is followed by the $E_g^{I,E(\uparrow/\downarrow)}$ one which is the width of the energy gap. For each quantity, we provide two values separated by a slash corresponding to the two spin directions. As it is obvious for the gapped metals the values for both spin directions are identical. Both $W_m^{I,E(\uparrow/\downarrow)}$ and $E_g^{I,E(\uparrow/\downarrow)}$ values are less than 1 eV and are comparable.

The rest twenty compounds under study are spin gapped materials as shown in Table 1. The ones with less than 18 valence electrons per unit cell have negative total spin magnetic moments per unit cell and are p-type spin gapped metals. The compounds with more than 18 valence electrons, on the other hand, have positive total spin magnetic moments and are n-type spin gapped metals. All n-type (p-type) spin gapped metals are not identical concerning their density of states. As shown in Table 1 there are several cases where the two spin band structures have a different character, *i.e.*, the one spin channel presents either a normal metallic (NM) or semiconducting (SC) behavior while the other spin channel presents a n(p)-type spin gapped metallic behavior. To make this clear, in Fig. 2 we have gathered the total DOS for some selected compounds and compared them with the schematic representations in Fig. 1. NiHfIn and NiHfSb are p-type and n-type gapped metals, respectively. FeTiSb presents p-type spin gapped metallic behavior for both spin directions. FeZrSb and FeVSn present p-type behavior for one spin direction and semiconducting (normal metallic) for the other. Similarly, PdTiSb, CoVSb and CuVSb present n-type spin gapped metallic behavior for one spin direction and n-type/semiconducting/normal-metallic behavior for the other spin direction. None of the studied compounds presents an electronic band structure similar to the j panel in Fig. 1, where one spin-band is n-type and the other is p-type. One could envisage that this behavior can be identified in another class of Heusler compounds like the equiatomic quaternary Heuslers since several of them are type-II spin-gapless semiconductors [64,65]. Actually in reference [66] (see Fig. 1), MnVTiAs compound combines a p-type gapped metallic behavior for the spin-up band structure with an n-type gapped metallic behavior for the spin-down electronic band structure. In that article, this behavior was referred to as "indirect spin-gapless semiconductors" since the concept of "spin gapped metals" was not known.

In Table 1, we have also included the atom-resolved spin magnetic moments for the two transition atoms in each compound, and the spin-polarization (SP) at the Fermi level. The atomic spin magnetic moments do not present any peculiarity. The transition metal atoms from Ti to Co are the ones carrying significant spin magnetic moments. On the other hand, the Ni/Cu atoms as well as the 4*d* and 5*d* transition metal atoms carry much smaller atomic spin magnetic moments. The SP at the Fermi level is defined as the difference between the number of spin-up $N^{\uparrow}(E_F)$ and spin-down $N^{\downarrow}(E_F)$ electronic states at the Fermi level divided by their sum, SP=$\frac{N^{\uparrow}(E_F)-N^{\downarrow}(E_F)}{N^{\uparrow}(E_F)+N^{\downarrow}(E_F)}$. The SP is positive in all cases and reaches an ideal 100% value when the spin-down electronic band is semiconducting.

As for the gapped metals, in Table 1 we also include the $W_m^{I,E(\uparrow/\downarrow)}$ and $E_g^{I,E(\uparrow/\downarrow)}$ values for the spin gapped metals. The slash in each case separates the values corresponding to the spin-up and spin-down band structures. In the case of normal metallic or usual semiconducting behavior for one spin band structure, the former quantities cannot be defined and thus are not provided. Both $W_m^{I,E(\uparrow/\downarrow)}$ and $E_g^{I,E(\uparrow/\downarrow)}$ values range in almost all cases between a few tenths of an eV up to 1 eV. It is worth noting that these values are very close to the energy gaps found in conventional semiconductors like Si, Ge or GaAs where the width of

the energy gap varies between ~0.5 eV and ~1.3 eV. Thus these spin gapped metals can be combined with conventional semiconductors in devices. Finally, the relative $W_{\mathrm{m}}^{\mathrm{I,E}(\uparrow/\downarrow)}$ and $E_{\mathrm{g}}^{\mathrm{I,E}(\uparrow/\downarrow)}$ widths are material's specific, as it can be deduced from Table 1, and no general rule can be drawn. This variety of values enhances the potential functionalities offered by the studied spin gapped metals.

Continuing our discussion on gapped metals and spin gapped metals, let us delve into their potential to revolutionize various electronic devices. These materials offer significant promise in addressing a major limitation of tunnel FETs and NDR tunnel diodes: band tails tunneling caused by doped semiconductor electrodes. Unlike their doped counterparts, gapped metals exhibit electronic behavior akin to intrinsic semiconductors, effectively mitigating this undesirable effect. This unique property paves the way for the development of high-performance, steep-slope tunnel FETs. As a concrete example, we can envision a design utilizing a p-type 17-valence electron half-Heusler compound as the source electrode, an 18-valence electron intrinsic semiconducting channel, and a 19-valence electron n-type half-Heusler compound as the drain electrode. Moreover, gapped metals offer exciting possibilities for novel FET designs beyond tunnel FETs. By leveraging both p-type (17-valence electron) and intrinsic (18-valence electron) half-Heusler compounds as source–drain electrodes and channel material, a new class of FETs can be realized. These devices not only exhibit conventional transistor functionality but also possess the novel gate-voltage tunable NDR effect. The external band gap $E_{\mathrm{g}}^{\mathrm{E}}$ of the p-type gapped metal, along with the bandwidth $W_{\mathrm{m}}^{\mathrm{E}}$, play a crucial role in determining the I-V characteristics of the FET and manifestation of the NDR effect. Note that this behavior, previously predicted in FETs based on cold metal source–drain electrodes [25], opens doors for innovative functionalities within a single device.

Finally, the potential of spin gapped metals extends far beyond the already impressive functionalities predicted for cold metals (or gapped metals) in devices like NDR tunnel diodes and steep-slope FETs [13]. However, the true power of these materials lies in their ability to exploit the spin degree of freedom, opening doors to entirely new functionalities. One exciting application would be replacing diluted magnetic semiconductors (DMS) in spin-Esaki diodes [67–72]. DMS are currently plagued by limitations such as low Curie temperature and difficulties in achieving high spin polarization. Spin gapped metals, on the other hand, offer the potential to overcome these limitations due to their intrinsic magnetic properties and unique band structures. Furthermore, spin gapped metals hold promise for realizing a new class of steep-slope spin FETs that can exhibit both non-local giant magnetoresistance (GMR) and NDR effect. This unique combination could revolutionize magnetic memory and logic concepts, paving the way for advancements in logic-in-memory computing.

3. Conclusions

In conclusion, gapped metals, a recently introduced category of materials, offer exciting possibilities for nanoelectronic devices. Their unique band structure allows them to behave intrinsically as p- or n-type semiconductors, eliminating the need for external doping. Building upon this concept, we have introduced the concept of "spin gapped metals", which exhibit independent p- or n-type character for each spin channel. This intrinsic magnetism, analogous to diluted magnetic semiconductors, eliminates the need for transition metal doping. Unlike gapped metals (or cold metals), spin gapped metals open doors to entirely new functionalities, including next-generation spintronic devices like spin-Esaki diodes and spin FETs with both non-local GMR effect and gate-voltage tunable NDR effect. To illustrate this concept, we employed first-principles electronic band structure calculations on half-Heusler compounds identified through the Open Quantum Materials Database. Our analysis, focusing on compounds with varying valence electron counts, revealed materials exhibiting both gapped metal and spin gapped metal behavior. This work highlights the transformative potential of spin gapped metals for materials design in next-generation spintronic and multifunctional devices. Further theoretical and experimental exploration is crucial to fully unlock the capabilities of this promising class of materials. Such studies could involve investigating their magnetic properties, transport characteristics, and device integration strategies.

CRediT authorship contribution statement

E. Şaşıoğlu: Writing – review & editing, Writing – original draft, Supervision, Project administration, Methodology, Data curation, Conceptualization. **M. Tas:** Investigation, Data curation. **S. Ghosh:** Visualization, Validation, Investigation, Data curation. **W. Beida:** Validation, Investigation, Formal analysis, Data curation. **B. Sanyal:** Project administration, Investigation, Conceptualization. **S. Blügel:** Writing – review & editing, Project administration, Investigation, Conceptualization. **I. Mertig:** Writing – review & editing, Project administration, Investigation, Conceptualization. **I. Galanakis:** Writing – review & editing, Writing – original draft, Supervision, Project administration, Formal analysis, Conceptualization.

Declaration of competing interest

The authors declare that they have no known competing financial interests or personal relationships that could have appeared to influence the work reported in this paper.

Acknowledgments

This work was supported by the European Union (EFRE) via grant No. ZS/2016/06/79307, the Federal Ministry of Education and Research of Germany (BMBF) in the framework of the Palestinian-German Science Bridge (BMBF grant number DBP01436), and the Deutsche Forschungsgemeinschaft (DFG) through the Collaborative Research Center SFB 1238 (Project C01) and SFB/TRR 227. M.T. acknowledges the TUBITAK ULAKBIM, High Performance and Grid Computing Center (TRUBA resources). B.S. acknowledges financial support from Swedish Research Council (grant No. 2022-04309 and grant No. 2018-07082). The computations were enabled by resources provided by the National Academic Infrastructure for Supercomputing in Sweden (NAISS) at NSC and PDC (NAISS 2024/3-40) partially funded by the Swedish Research Council through grant agreement No. 2022-06725.

Data availability

Data will be made available on request.

References

[1] L.E. Bell, Cooling, heating, generating power, and recovering waste heat with thermoelectric systems, Science 321 (2008) 1457, http://dx.doi.org/10.1126/science.115889.

[2] D. Champier, Thermoelectric generators: a review of applications, Energy Convers. Manage. 140 (2017) 167, http://dx.doi.org/10.1016/j.enconman.2017.02.070.

[3] F. Ricci, A. Dunn, A. Jain, G.-M. Rignanese, G. Hautier, Gapped metals as thermoelectric materials revealed by high-throughput screening, J. Mater. Chem. A 8 (2020) 17579, http://dx.doi.org/10.1039/d0ta05197g.

[4] O.I. Malyi, A. Zunger, False metals, real insulators, and degenerate gapped metals, Appl. Phys. Rev. 7 (2020) 041310, http://dx.doi.org/10.1063/5.0015322.

[5] M.R. Khan, H.R. Gopidi, O.I. Malyia, Optical properties and electronic structures of intrinsic gapped metals: Inverse materials design principles for transparent conductors, Appl. Phys. Lett. 123 (2023) 061101, http://dx.doi.org/10.1063/5.0153382.

[6] A.L. Efros, Density of states and interband absorption of light in strongly doped semiconductors, Sov. Phys. Uspekhi 16 (6) (1974) 789, http://dx.doi.org/10.1070/PU1974v016n06ABEH004090.

[7] P.K. Chakraborty, K.P. Ghatak, On the density-of-states function in heavily doped compound semiconductors, Phys. Lett. A 288 (5–6) (2001) 335–339, http://dx.doi.org/10.1016/S0375-9601(01)00513-8.

[8] E.O. Kane, Band tails in semiconductors, Solid State Electron. 28 (1–2) (1985) 3–10, http://dx.doi.org/10.1016/0038-1101(85)90203-5.

[9] P. Van Mieghem, Theory of band tails in heavily doped semiconductors, Rev. Modern Phys. 64 (3) (1992) 755, http://dx.doi.org/10.1103/RevModPhys.64.755.

[10] S. Sant, A. Schenk, The effect of density-of-state tails on band-to-band tunneling: Theory and application to tunnel field effect transistors, J. Appl. Phys. 122 (13) (2017) 135702, http://dx.doi.org/10.1063/1.4994112.

[11] J. Bizindavyi, A.S. Verhulst, Q. Smets, D. Verreck, B. Sorée, G. Groeseneken, Band-tails tunneling resolving the theory-experiment discrepancy in esaki diodes, IEEE J. Electron Devices Soc. 6 (2018) 633–641, http://dx.doi.org/10.1109/JEDS.2018.2834825.

[12] A. Schenk, S. Sant, Tunneling between density-of-state tails: Theory and effect on esaki diodes, J. Appl. Phys. 128 (1) (2020) 014502, http://dx.doi.org/10.1063/5.0008709.

[13] S. Wang, J. Wang, T. Zhi, J. Xue, D. Chen, L. Wang, R. Zhang, Cold source field-effect transistors: Breaking the 60-mV/decade switching limit at room temperature, Phys. Rep. 1013 (2023) 1–33, http://dx.doi.org/10.1016/j.physrep.2023.03.001.

[14] E. Şaşıoğlu, I. Mertig, Theoretical prediction of semiconductor-free negative differential resistance tunnel diodes with high peak-to-valley current ratios based on two-dimensional cold metals, ACS Appl. Nano Mater. 6 (5) (2023) 3758–3766, http://dx.doi.org/10.1021/acsanm.2c05478.

[15] C. Qiu, F. Liu, L. Xu, B. Deng, M. Xiao, J. Si, L. Lin, Z. Zhang, J. Wang, H. Guo, H. Peng, L.-M. Peng, Dirac-source field-effect transistors as energy-efficient, high-performance electronic switches, Science 361 (6400) (2018) 387–392, http://dx.doi.org/10.1126/science.aap9195.

[16] F. Liu, Switching at less than 60 mv/decade with a "cold" metal as the injection source, Phys. Rev. Appl. 13 (6) (2020) 064037, http://dx.doi.org/10.1103/PhysRevApplied.13.064037.

[17] E.G. Marin, D. Marian, M. Perucchini, G. Fiori, G. Iannaccone, Lateral heterostructure field-effect transistors based on two-dimensional material stacks with varying thickness and energy filtering source, ACS Nano 14 (2) (2020) 1982–1989, http://dx.doi.org/10.1021/acsnano.9b08489.

[18] D. Logoteta, J. Cao, M. Pala, P. Dollfus, Y. Lee, G. Iannaccone, Cold-source paradigm for steep-slope transistors based on van der waals heterojunctions, Phys. Rev. Res. 2 (4) (2020) 043286, http://dx.doi.org/10.1103/PhysRevResearch.2.043286.

[19] Z. Tang, C. Liu, X. Huang, S. Zeng, L. Liu, J. Li, Y.-G. Jiang, D.W. Zhang, P. Zhou, A steep-slope MoS_2/graphene Dirac-source field-effect transistor with a large drive current, Nano Lett. 21 (4) (2021) 1758–1764, http://dx.doi.org/10.1021/acs.nanolett.0c04657.

[20] W. Shin, G. Myeong, K. Sung, S. Kim, H. Lim, B. Kim, T. Jin, J. Park, K. Watanabe, T. Taniguchi, F. Liu, S. Cho, Steep-slope Schottky diode with cold metal source, Appl. Phys. Lett. 120 (24) (2022) 243506, http://dx.doi.org/10.1063/5.0097408.

[21] K. Sato, L. Bergqvist, J. Kudrnovský, P.H. Dederichs, O. Eriksson, I. Turek, B. Sanyal, G. Bouzerar, H. Katayama-Yoshida, V.A. Dinh, T. Fukushima, H. Kizaki, R. Zeller, First-principles theory of dilute magnetic semiconductors, Rev. Modern Phys. 82 (2010) 1633, http://dx.doi.org/10.1103/RevModPhys.82.1633.

[22] B.-H. Lei, D.J. Singh, Computational search for itinerant n-type and p-type magnetic semiconductors: Arsenopyrites as bipolar magnetic semiconductors, Phys. Rev. B 105 (2022) L121201, http://dx.doi.org/10.1103/PhysRevB.105.L121201.

[23] N.T. Tu, P.N. Hai, L.D. Anh, M. Tanaka, (Ga,Fe)Sb: A p-type ferromagnetic semiconductor, Appl. Phys. Lett. 105 (2014) 132402, http://dx.doi.org/10.1063/1.4896539.

[24] K. Kroth, B. Balke, G.H. Fecher, V. Ksenofontov, C. Felser, H.-J. Lin, Diluted magnetic semiconductors with high curie temperature based on C1(b) compounds: $CoTi_{1-x}Fe_xSb$, Appl. Phys. Lett. 89 (2006) 202509, http://dx.doi.org/10.1063/1.2388876.

[25] Y. Yin, Z. Zhang, C. Shao, J. Robertson, Y. Guo, Computational study of transition metal dichalcogenide cold source MOSFETs with sub-60 mV per decade and negative differential resistance effect, Npj 2D Mater. Appl. 6 (1) (2022) 55, http://dx.doi.org/10.1038/s41699-022-00332-6.

[26] R. Sakuma, P. Werner, F. Aryasetiawan, Electronic structure of $SrVO_3$ within GW+DMFT, Phys. Rev. B 88 (23) (2013) 235110, http://dx.doi.org/10.1103/PhysRevB.88.235110.

[27] C. Bigi, P. Orgiani, J. Sławińska, J. Fujii, J.T. Irvine, S. Picozzi, G. Panaccione, I. Vobornik, G. Rossi, D. Payne, et al., Direct insight into the band structure of $SrNbO_3$, Phys. Rev. Mater. 4 (2) (2020) 025006, http://dx.doi.org/10.1103/PhysRevMaterials.4.025006.

[28] A.F. May, D.J. Singh, G.J. Snyder, Influence of band structure on the large thermoelectric performance of lanthanum telluride, Phys. Rev. B 79 (15) (2009) 153101, http://dx.doi.org/10.1103/PhysRevB.79.153101.

[29] L. Huang, R. He, S. Chen, H. Zhang, K. Dahal, H. Zhou, H. Wang, Q. Zhang, Z. Ren, A new n-type half-Heusler thermoelectric material nbcosb, Mater. Res. Bull. 70 (2015) 773–778, http://dx.doi.org/10.1016/j.materresbull.2015.06.022.

[30] E. Gürbüz, S. Ghosh, E. Şaşıoğlu, I. Galanakis, I. Mertig, B. Sanyal, Spin-polarized two-dimensional electron/hole gas at the interface of nonmagnetic semiconducting half-Heusler compounds: Modified Slater-Pauling rule for half-metallicity at the interface, Phys. Rev. Mater. 7 (2023) 054405, http://dx.doi.org/10.1103/PhysRevMaterials.7.054405.

[31] J. Ma, V.I. Hegde, K. Munira, Y. Xie, S. Keshavarz, D.T. Mildebrath, C. Wolverton, A.W. Ghosh, W.H. Butler, Computational investigation of half-Heusler compounds for spintronics applications, Phys. Rev. B 95 (2017) 024411, http://dx.doi.org/10.1103/PhysRevB.95.024411.

[32] D. Jung, H.-J. Koo, M.-H. Whangbo, Study of the 18-electron band gap and ferromagnetism in semi-Heusler compounds by non-spin-polarized electronic band structure calculations, J. Mol. Struct.: THEOCHEM 527 (2000) 113, http://dx.doi.org/10.1016/S0166-1280(00)00483-8.

[33] J. Pierre, R.V. Skolozdra, Y.K. Gorelenko, M. Kouacou, From nonmagnetic semiconductor to itinerant ferromagnet in the TiNiSn-TiCoSn series, J. Magn. Magn. Mater. 134 (1994) 95–105, http://dx.doi.org/10.1016/0304-8853(94)90078-7.

[34] J. Tobola, J. Pierre, Electronic phase diagram of the XTZ (X=Fe, Co, Ni; T=Ti, V, Zr, Nb, Mn; Z=Sn, Sb) semi-Heusler compounds, J. Alloys Compd. 296 (2000) 243–252, http://dx.doi.org/10.1016/S0925-8388(99)00549-6.

[35] S. Ouardi, G.H. Fecher, C. Felser, M. Schwall, S.S. Naghavi, A. Gloskovskii, B. Balke, J. Hamrle, K. Postava, J. Pištora, S. Ueda, K. Kobayashi, Electronic structure and optical, mechanical, and transport properties of the pure, electron-doped, and hole-doped Heusler compound CoTiSb, Phys. Rev. B 86 (2012) 045116, http://dx.doi.org/10.1103/PhysRevB.86.045116.

[36] M. Mokhtari, F. Dahmane, G. Benabdellah, L. Zekri, S. Benalia, N. Zekri, Theoretical study of the structural stability, electronic and magnetic properties of XVSb ((X=Fe, Co, and Ni) half-Heusler compounds, Condens. Matter Phys. 11 (2018) 43705, http://dx.doi.org/10.5488/CMP.21.43705.

[37] E. Gürbüz, M. Tas, E. Şaşıoğlu, I. Mertig, B. Sanyal, I. Galanakis, First-principles prediction of energy bandgaps in 18-valence electron semiconducting half-Heusler compounds: Exploring the role of exchange and correlation, J. Appl. Phys. 134 (2023) 205703, http://dx.doi.org/10.1063/5.0178165.

[38] G. Xu, E.K. Liu, Y. Du, G.J. Li, G.D. Liu, W.H. Wang, G.H. Wu, New spin gapless semiconductors family: Quaternary Heusler compounds, Europhys. Lett. 102 (2013) 17007, http://dx.doi.org/10.1209/0295-5075/102/17007.

[39] URL https://oqmd.org/.

[40] J. Saal, S. Kirklin, M. Aykol, B. Meredig, C. Wolverton, Materials Design and Discovery with High-Throughput Density Functional Theory: The Open Quantum Materials Database (OQMD), JOM 65 (2013) 1501, http://dx.doi.org/10.1007/s11837-013-0755-4.

[41] S. Kirklin, J. Saal, B. Meredig, A. Thompson, J. Doak, M. Aykol, S. Rühl, C. Wolverton, The Open Quantum Materials Database (OQMD): assessing the accuracy of DFT formation energies, Npj Comput. Mater. 1 (2015) 15010, http://dx.doi.org/10.1038/npjcompumats.2015.10.

[42] T. Graf, C. Felser, S.S.P. Parkin, Simple rules for the understanding of Heusler compounds, Progr. Sol. St. Chem. 39 (2011) 1–50, http://dx.doi.org/10.1016/j.progsolidstchem.2011.02.001.

[43] S. Tavares, K. Yang, M.A. Meyers, Heusler alloys: Past, properties, new alloys, and prospects, Progr. Mat. Sci. 132 (2023) 101017, http://dx.doi.org/10.1016/j.pmatsci.2022.101017.

[44] S. Chatterjee, S. Chatterjee, S. Giri, S. Majumdar, Transport properties of Heusler compounds and alloys, J. Phys.: Condens. Matter. 34 (2022) 013001, http://dx.doi.org/10.1088/1361-648X/ac268c.

[45] I. Galanakis, Slater-Pauling behavior in half-metallic Heusler compounds, Nanomaterials 13 (2023) 2010, http://dx.doi.org/10.3390/nano13132010.

[46] S. Ouardi, G.H. Fecher, C. Felser, J. Kübler, Realization of spin gapless semiconductors: The Heusler compound Mn_2CoAl, Phys. Rev. Lett. 110 (2013) 100401, http://dx.doi.org/10.1103/PhysRevLett.110.100401.

[47] Q. Gao, I. Opahle, H. Zhang, High-throughput screening for spin-gapless semiconductors in quaternary Heusler compounds, Phys. Rev. Mater. 3 (2019) 024410, http://dx.doi.org/10.1103/PhysRevMaterials.3.024410.

[48] I. Galanakis, K. Özdoğan, E. Şaşıoğlu, Spin-filter and spin-gapless semiconductors: The case of Heusler compounds, AIP Adv. 6 (2016) 055606, http://dx.doi.org/10.1063/1.4943761.

[49] M. Gilleßen, R. Dronskowski, A combinatorial study of full Heusler alloys by first-principles computational methods, J. Comput. Chem. 30 (2009) 1290, http://dx.doi.org/10.1002/jcc.21152.

[50] M. Gilleßen, R. Dronskowski, A combinatorial study of inverse Heusler alloys by first-principles computational methods, J. Comput. Chem. 31 (2010) 612, http://dx.doi.org/10.1002/jcc.21358.

[51] S.V. Faleev, Y. Ferrante, J. Jeong, M.G. Samant, B. Jones, S.S.P. Parkin, Unified explanation of chemical ordering, the Slater-Pauling rule, and half-metallicity in full Heusler compounds, Phys. Rev. B 95 (2017) 045140, http://dx.doi.org/10.1103/PhysRevB.95.045140.

[52] S.V. Faleev, Y. Ferrante, J. Jeong, M.G. Samant, B. Jones, S.S.P. Parkin, Origin of the tetragonal ground state of Heusler compounds, Phys. Rev. Appl. 7 (2017) 034022, http://dx.doi.org/10.1103/PhysRevApplied.7.034022.

[53] S.V. Faleev, Y. Ferrante, J. Jeong, M.G. Samant, B. Jones, S.S.P. Parkin, Heusler compounds with perpendicular magnetic anisotropy and large tunneling magnetoresistance, Phys. Rev. Mater. 1 (2017) 024402, http://dx.doi.org/10.1103/PhysRevMaterials.1.024402.

[54] M. Marathe, H.C. Herper, Exploration of all-3d Heusler alloys for permanent magnets: An ab initio based high-throughput study, Phys. Rev. B 107 (2023) 174402, http://dx.doi.org/10.1103/PhysRevB.107.174402.

[55] S. Sanvito, J. Xue, A. Tiwari, M. Zic, T. Archer, P. Tozman, M. Venkatesan, M. Coey, S. Curtarolo, Accelerated discovery of new magnets in the Heusler alloy family, Sci. Adv. 3 (2017) e1602241, http://dx.doi.org/10.1126/sciadv.1602241.

[56] J.P. Perdew, K. Burke, M. Ernzerhof, Generalized gradient approximation made simple, Phys. Rev. Lett. 77 (1996) 3865–3868, http://dx.doi.org/10.1103/PhysRevLett.77.3865.

[57] S. Smidstrup, D. Stradi, J. Wellendorff, P.A. Khomyakov, U.G. Vej-Hansen, M.-E. Lee, T. Ghosh, E. Jónsson, H. Jónsson, K. Stokbro, First-principles Green's-function method for surface calculations: A pseudopotential localized basis set approach, Phys. Rev. B 96 (2017) 195309, http://dx.doi.org/10.1103/PhysRevB.96.195309.

[58] S. Smidstrup, T. Markussen, P. Vancraeyveld, J. Wellendorff, J. Schneider, T. Gunst, B. Verstichel, D. Stradi, P.A. Khomyakov, U.G. Vej-Hansen, M.-E. Lee, S.T. Chill, F. Rasmussen, G. Penazzi, F. Corsetti, A. Ojanpera, K. Jensen, M.L.N. Palsgaard, U. Martinez, A. Blom, M. Brandbyge, K. Stokbro, QuantumATK: an integrated platform of electronic and atomic-scale modelling tools, J. Phys.: Condens. Matter. 32 (2020) 015901, http://dx.doi.org/10.1088/1361-648X/ab4007.

[59] M.J. van Setten, M. Giantomassi, E. Bousquet, M.J. Verstraete, D.R. Hamann, X. Gonze, G.M. Rignanese, The PSEUDODOJO: Training and grading a 85 element optimized norm-conserving pseudopotential table, Comp. Phys. Commun. 226 (2018) 39–54, http://dx.doi.org/10.1016/j.cpc.2018.01.012.

[60] M. Meinert, Modified Becke-Johnson potential investigation of half-metallic Heusler compounds, Phys. Rev. B 87 (2013) 045103, http://dx.doi.org/10.1103/PhysRevB.87.045103.

[61] H.J. Monkhorst, J.D. Pack, Special points for Brillouin-zone integrations, Phys. Rev. B 13 (1976) 5188, http://dx.doi.org/10.1103/PhysRevB.13.5188.

[62] P. Mavropoulos, K. Sato, R. Zeller, P. Dederichs, V. Popescu, H. Ebert, Effect of the spin-orbit interaction on the band gap of half metals, Phys. Rev. B 69 (2004) 054424, http://dx.doi.org/10.1103/PhysRevB.69.054424.

[63] P. Mavropoulos, I. Galanakis, V. Popescu, P. Dederichs, The influence of spin–orbit coupling on the band gap of Heusler alloys, J. Phys.: Condens. Matter. 16 (2004) S5759, http://dx.doi.org/10.1088/0953-8984/16/48/043.

[64] Q. Gao, I. Opahle, H. Zhang, High-throughput screening for spin-gapless semiconductors in quaternary Heusler compounds, Phys. Rev. Mater. 3 (2019) 024410, http://dx.doi.org/10.1103/PhysRevMaterials.3.024410.

[65] T. Aull, E. Şaşıoğlu, I.V. Maznichenko, S. Ostanin, A. Ernst, I. Mertig, I. Galanakis, Ab initio design of quaternary Heusler compounds for reconfigurable magnetic tunnel diodes and transistors, Phys. Rev. Mater. 3 (2019) 124415, http://dx.doi.org/10.1103/PhysRevMaterials.3.124415.

[66] K. Özdoğan, E. Şaşıoğlu, I. Galanakis, Slater-Pauling behavior in LiMgPdSn-type multifunctional quaternary Heusler materials: Half-metallicity, spin-gapless and magnetic semiconductors, J. Appl. Phys. 113 (2013) 193903, http://dx.doi.org/10.1063/1.4805063.

[67] M. Kohda, Y. Ohno, K. Takamura, F. Matsukura, H. Ohno, A spin esaki diode, Japan. J. Appl. Phys. 40 (12A) (2001) L1274, http://dx.doi.org/10.1143/JJAP.40.L1274.

[68] A. Einwanger, M. Ciorga, U. Wurstbauer, D. Schuh, W. Wegscheider, D. Weiss, Tunneling anisotropic spin polarization in lateral (Ga,Mn)As/GaAs spin Esaki diode devices, Appl. Phys. Lett. 95 (15) (2009) http://dx.doi.org/10.1063/1.3247187.

[69] M. Kohda, T. Kita, Y. Ohno, F. Matsukura, H. Ohno, Bias voltage dependence of the electron spin injection studied in a three-terminal device based on a (Ga, Mn) As/ n^+-GaAs Esaki diode, Appl. Phys. Lett. 89 (1) (2006) http://dx.doi.org/10.1063/1.2219141.

[70] L.D. Anh, P.N. Hai, M. Tanaka, Observation of spontaneous spin-splitting in the band structure of an n-type zinc-blende ferromagnetic semiconductor, Nat. Commun. 7 (1) (2016) 13810, http://dx.doi.org/10.1038/ncomms13810.

[71] L.D. Anh, P.N. Hai, M. Tanaka, Electrical tuning of the band alignment and magnetoconductance in an n-type ferromagnetic semiconductor (In, Fe) As-based spin-Esaki diode, Appl. Phys. Lett. 112 (10) (2018) http://dx.doi.org/10.1063/1.5010020.

[72] T. Arakawa, J. Shiogai, M. Maeda, M. Ciorga, M. Utz, D. Schuh, Y. Niimi, M. Kohda, J. Nitta, D. Bougeard, et al., Tunneling mechanism in a (Ga, Mn) As/GaAs-based spin Esaki diode investigated by bias-dependent shot noise measurements, Phys. Rev. B 102 (4) (2020) 045308, http://dx.doi.org/10.1103/PhysRevB.102.045308.